Published by Fusion Energy Division, Oak Ridge National Laboratory
Building 9201-2 P.O. Box 2009 Oak Ridge, TN 37831-8071, USA

Editor: James A. Rome Issue 76 July 2001
E-Mail: jar@ornl.gov Phone (865) 574-1306
On the Web at *http://www.ornl.gov/fed/stelnews*

First plasma results from HSX

HSX is a quasihelically symmetric (QHS) stellarator with virtually no toroidal curvature. This quasi-symmetry is predicted to result in good confinement of deeply trapped particles and very low neoclassical transport. A set of auxiliary coils can be used to introduce a toroidal mirror term ($n = 4$, $m = 0$) into the magnetic field spectrum; this spoils the symmetry and can lead to the direct loss of trapped particles at low collisionality.

Experimental operations have begun using 28-GHz second harmonic electron cyclotron resonance heating (ECRH) at $B = 0.5$ T to create a deeply trapped energetic electron population. The ECRH is introduced from the low-field side through an ellipsoidal focusing mirror, giving a spot size of ~4 cm at the magnetic axis. Initial studies examined the breakdown time of the plasma. At fixed neutral density (gas puff) and rf power, the time to reach a small but measurable density, defined as the breakdown time, is a measure of how well the ionizing electrons are confined. Figure 1 shows the time between application of the ECRH and the attainment of a line-averaged central density of 2×10^{11} cm^{-3}, plotted as a function of r/a (of the resonance location) from the magnetic axis. Data for operation of HSX in the QHS mode are plotted as triangles, data for the mirror mode as stars, and data for a "deeper" mirror mode (with phasing opposite to that of the conventional mirror mode) as squares. For all cases, the breakdown time is a minimum with the resonance on axis. The QHS data show symmetry about the axis, indicating that the breakdown time depends only on the flux surface where the microwaves are resonant. Breakdown times on the high-field side of the torus are comparable for all three cases. As the resonance is moved to the low-field side of the torus, where trapped particles play a significant role, the breakdown times increase significantly as the deviation from symmetry increases.

Prior to vessel conditioning, the electron density rose uncontrollably until reaching cut-off (4.9×10^{12} cm^{-3}) followed by a thermal collapse. After extensive wall conditioning with hydrogen and helium glow, controlled low-

In this issue . . .

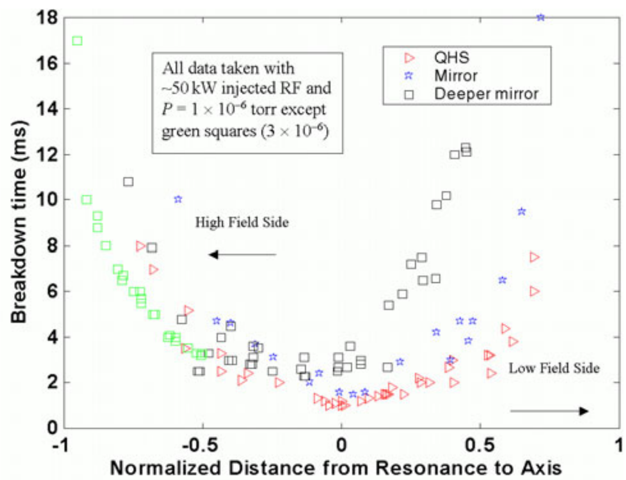

Fig. 1. Time after application of ECRH to reach a line-averaged density of 2×10^{11} cm^{-3}, as a function of resonance location with respect to the magnetic axis at the ECRH launch position. Minimum breakdown for all cases is with on-axis heating. The time to reach a significant breakdown increases with low-field side heating with broken symmetry.

density discharges (2×10^{11} cm^{-3} to 2×10^{12} cm^{-3}) can now be routinely produced.

Low-density discharges have been formed with ~50 kW of injected ECRH power in both the QHS and mirror modes with central resonance heating. Figure 2 shows the central line-averaged density and the stored energy (from a diamagnetic loop) for the QHS configuration (top) and for the mirror mode (bottom). For the QHS configuration, the stored energy is seen to rise continuously from the onset of heating (at $t = 0.800$ s) throughout the discharge until the ECRH is terminated (at 0.825 seconds). The absorbed power at the end of the discharge is estimated from the change in slope of the stored energy just before, and immediately after, the ECRH is turned off. These estimates give ~15 kW, or ~30% of the injected power. Confinement times estimated from the absorbed power and stored energy are about 2 ms. For the mirror mode, the stored energy quickly saturates at a level about 20% that of the QHS case, with confinement times on the order of 1 ms.

Highly peaked density profiles are observed for the QHS mode of operation, and broadened ones for the deep mirror mode. Thomson scattering and electron cyclotron emission (ECE) diagnostics will not be available on HSX until later this calendar year, but some estimates of the electron temperature can be made based on a soft x-ray (S-X) triplet that is well collimated on the magnetic axis with three different foil thicknesses. For discharges with a line-averaged density of 1×10^{12} cm^{-3} (where we get sufficient signal for the S-X system), T_{e0} inferred from the S-X system is ~1500 eV. Because of the low density of operation, this

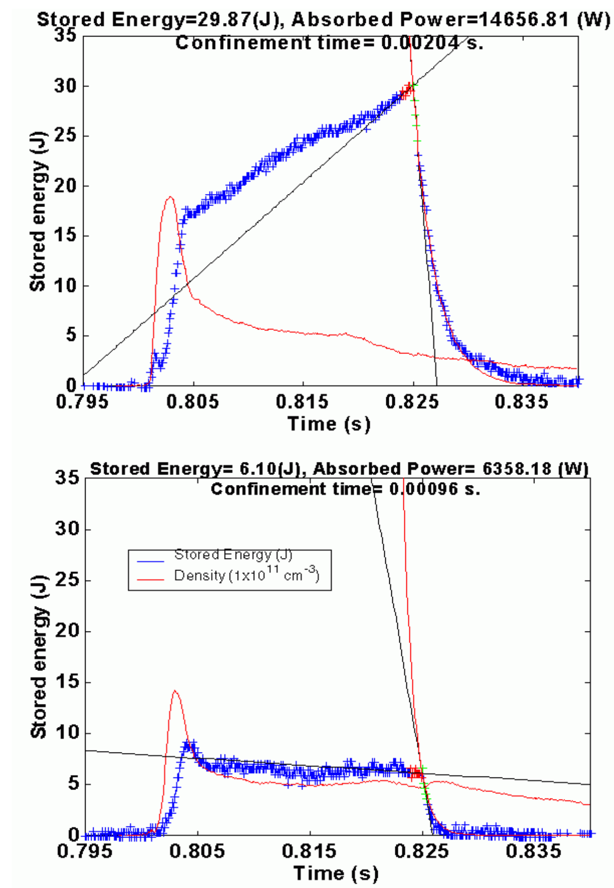

Fig. 2. Stored energy in the QHS configuration (top) and mirror mode configuration (bottom) as a function of time. In both cases, 50 kW of launched ECRH was applied with central resonance from 0.800 to 0.825 s with line-averaged density controlled to ~5×10^{11} cm^{-3}. Absorbed power was inferred from the change in stored energy with rapid ECRH turn-off.

energetic component is well into the long mean-free-path regime.

We have measured the stored energy in QHS and mirror mode discharges as a function of the resonance location. Figure 3 shows a plot of the stored energy, averaged over several discharges during which the density was held stationary at 1×10^{12} cm^{-3}. For the QHS case we see that the stored energy peaks with the resonance on axis and is reasonably symmetric with respect to high-field side/low-field side heating. For the mirror mode, similar values of stored energy are observed with high-field side heating, but the stored energy quickly drops as the resonance is moved to the low-field side, exhibiting a strong asymmetry.

Figure 4 shows a comparison of the stored energy in the QHS and mirror modes with on-axis resonance as a function of the central line-averaged density. While there is some scatter in the QHS data, the stored energy appears

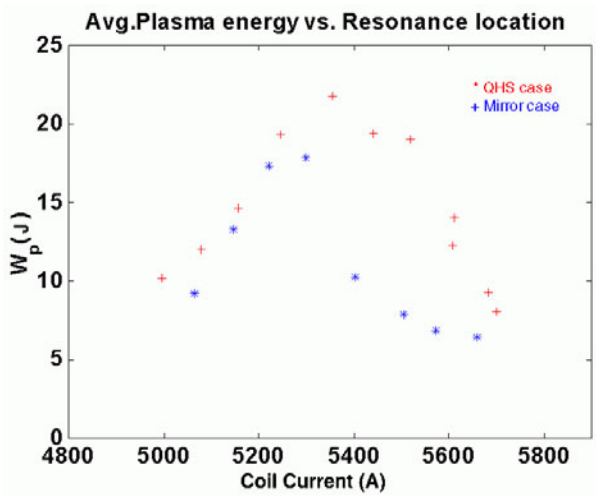

Fig. 3. Stored energy as a function of resonance location for the QHS configuration compared to the mirror mode. Line-averaged density controlled to 1×10^{12} cm^{-3}.

nearly constant, or perhaps has a slight decreasing tendency. For the mirror case, on the other hand, the stored energy is clearly dependent on the density, rising nearly a factor of 3 over the range. With increasing collisionality, the stored energy in the mirror configuration becomes roughly comparable to that in the QHS configuration.

These initial results from HSX using second harmonic ECRH at low plasma density to create energetic trapped electrons point to clear beneficial effects of symmetry on the plasma breakdown, energy content, and confinement. These initial studies will be refined and investigated in more detail as additional diagnostics become available.

David T. Anderson for the HSX Team
HSX Laboratory
University of Wisconsin, Madison
1415 Engineering Drive, Madison, WI 53706
E-mail: dtanders@facstaff.wisc.edu

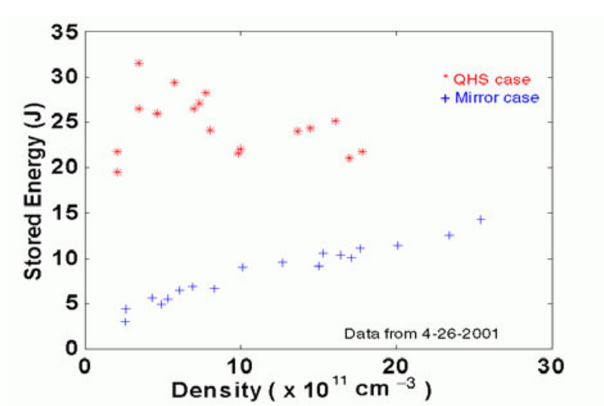

Fig. 4. Stored energy as a function of line-averaged density for the QHS and mirror modes of operation with central ECRH resonance.

Design of the National Compact Stellarator Experiment

A new stellarator facility, the National Compact Stellarator Experiment (NCSX), is being designed as part of a U.S. program proposed [1] to develop the physics of compact stellarators, an innovative magnetic plasma confinement concept for fusion. Most of the magnetic confinement research to date has concentrated on tokamaks and stellarators. Tokamaks have demonstrated excellent short-pulse plasma performance in “compact” geometries, with aspect ratios (ratio of the plasma major radius to the average minor radius) usually less than 4. Stellarators have demonstrated levels of performance approaching those of tokamaks, generally at aspect ratios in the range of 6–12. The NCSX is designed to build on the advances in stellarators and tokamaks and to combine their best features. It takes advantage of the tokamak’s excellent confinement, ability to stabilize and manipulate turbulent transport, and lower aspect ratio (compared to classical stellarators) to reduce development costs and system size. It uses the stellarator’s externally generated helical field and three-dimensional shaping flexibility to passively stabilize the magnetohydrodynamic (MHD) modes (particularly the external kink and neoclassical tearing modes) that limit the pressure and pulse length in tokamak plasmas. These stellarator features make it possible to test the compact stellarator’s potential to provide a disruption-free plasma that can be steady state without external current drive or feedback systems.

The NCSX design uses the quasi-axisymmetric stellarator (QAS) concept, which is based upon work by A. Boozer [2], J. Nührenberg [3], and P. Garabedian [4] showing that stellarators, while 3-D in Euclidean space, can be designed to improve drift-orbit confinement by providing a direction of approximate symmetry of $|\boldsymbol{B}|$ in (Boozer) flux coordinates. The QAS design, in which the symmetry direction is toroidal (as in tokamaks), provides adequate fast ion confinement and low neoclassical transport losses, allows undamped flows to stabilize turbulence, allows self-generated bootstrap currents to generate some of the rotational transform, and is best suited for merging tokamak and stellarator physics.

Mission and physics design

The NCSX will support experiments to investigate the effects of 3-D plasma shaping, of internally and externally generated sources of rotational transform, and of quasi-axisymmetry on the stability and confinement of toroidal plasmas. It is designed to provide unique capabilities for broadening physics understanding for toroidal confine-

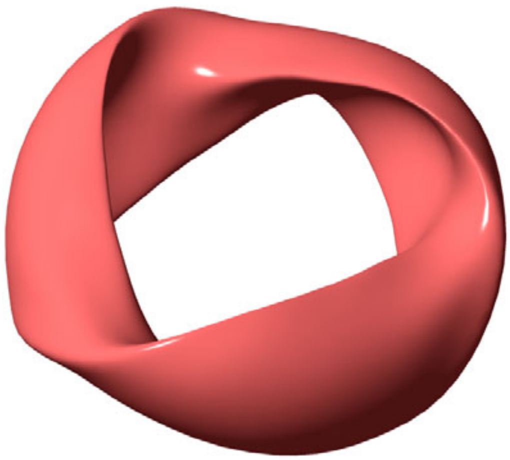

Fig. 1. NCSX reference plasma configuration

ment generally, and to acquire physics data needed to evaluate the attractiveness of the compact stellarator as a concept for fusion energy. Research on NCSX is needed to weigh the physics benefits of compact stellarators, passive stability and tokamak-like confinement, including the ability to manipulate the turbulent transport with flows, against the costs associated with more complex coils.

In order to carry out this mission, the NCSX has been designed around a computed QAS plasma configuration (Fig. 1). It has three periods, an aspect ratio $R/\langle a\rangle = 4.4$, strong axisymmetric shaping (average elongation ~1.8), and three-dimensional shaping as shown in the figure. The shape is optimized for good quasi-axisymmetry, good magnetic surfaces, and marginal stability to ballooning, external kink, vertical, and Mercier modes at $\beta = 4\%$. The rotational transform profile (Fig. 2) increases monotonically, except very near the edge, from about 0.4 ($q \sim 2.5$) to 0.65 ($q \sim 1.5$). The bootstrap current provides about one-fourth of the rotational transform at the edge, while the remainder is provided by coils. The high degree of quasiaxisymmetry is characterized by the very low effective helical ripple $\varepsilon_{h,eff}$ (Fig. 3), calculated numerically to match the low-collisionality transport regime [5]. The plasma as designed has good magnetic surfaces all the way to the edge except for a small island chain at the $\bar{\iota} = 0.6$ surface, which is removed by boundary perturbations that are small enough not to affect the transport and stability properties.

The main coils for NCSX are the 21 modular coils shown in Fig. 4. Three of the coils are extended radially to allow tangential access for neutral beams and diagnostics. Not shown but also included are a set of weak toroidal field coils, poloidal field coils, and trim coils for configuration flexibility. The coils are designed to reconstruct the physics properties of the reference plasma and to provide experimental flexibility to test the physics, for example the ability to vary the rotational transform, the shear, and the

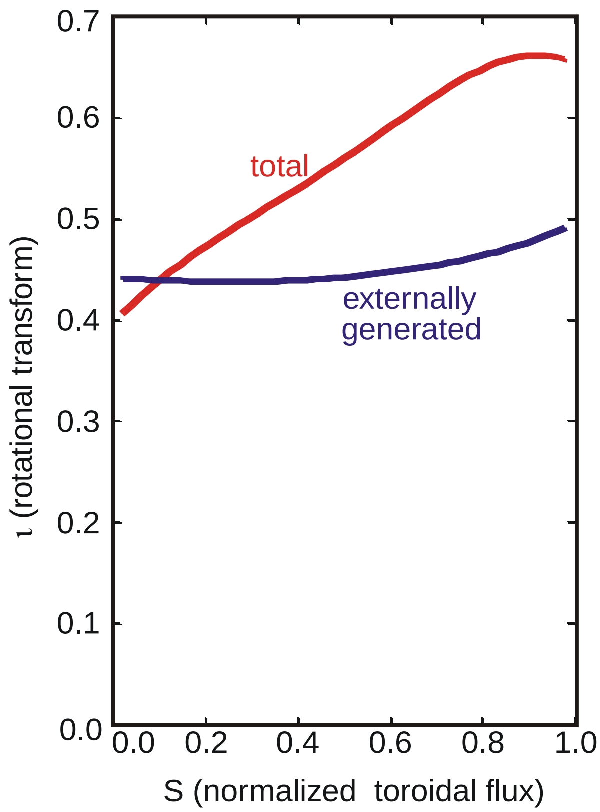

Fig. 2. Rotational transform profile and its externally generated component.

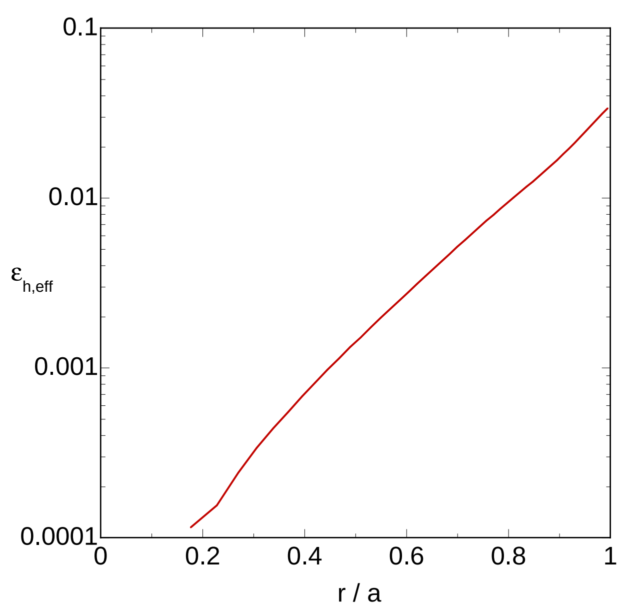

Fig. 3. Radial profile of NCSX effective helical ripple.

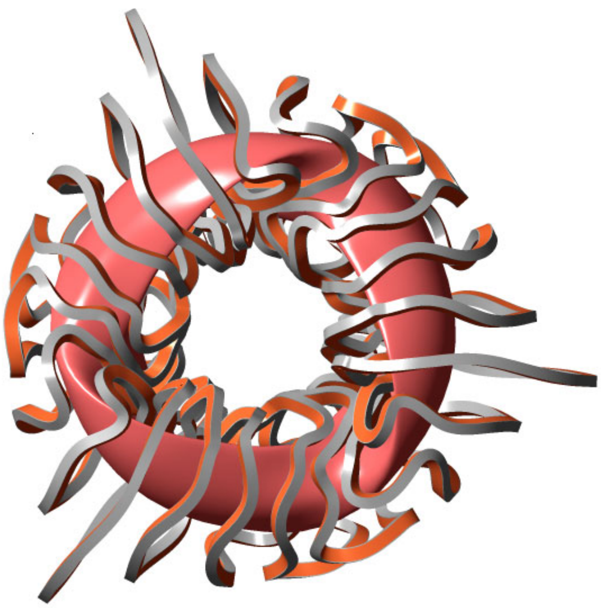

Fig. 4. NCSX modular coils.

stability beta limit, while maintaining good quasi-symmetry. The design is robust in that the coils can provide good configuration properties over a wide range of β, I_P, and profile shapes. Startup simulations have been carried out, demonstrating the evolution from an initial vacuum state to a high-beta target state along a stable path, consistent with planned equipment capabilities. Residual islands are eliminated using a methodology similar to the fixed-boundary technique described above to reduce calculated island widths in free-boundary equilibria by making small resonant perturbations in the coil geometry. The resulting coils are able to produce good magnetic surfaces over a wide range of conditions. (Fig. 5). A system of trim coils is included in the design to provide a capability for reducing islands over the range of equilibria needed for startup and flexibility. As a further measure the configuration is designed with "reversed shear" so that neoclassical effects should reduce the widths of any islands.

The NCSX will have a major radius of 1.4 m and a magnetic field (*B*) range of 1.2–1.7 T in the nominal configuration (>2 T at reduced rotational transform). Transport predictions based on these machine parameters indicate that plasmas with β = 4%, ν* = 0.25, *B* = 1.2 T, and average density 6×10^{19} m^{-3} can be realized with 6 MW of neutral beam injected power. This requires a global confinement time 2.9 times the ISS95 scaling, somewhat higher than the best achieved on LHD and W7-AS, or 0.9 times the ITER-97P tokamak H-mode scaling, using the current required to match the stellarator edge rotational transform in a tokamak with the same average shape.

A total of 12 MW of auxiliary heating can be accommodated in the NCSX design, 6 MW of tangential neutral beam injection (NBI) and 6 MW of radiofrequency (rf) heating. Initially the facility will be equipped with 3 MW of tangential NBI using two of the four existing PBX-M neutral beam lines arranged in a balanced (1 co, 1 counter) configuration. The remaining two can be added to upgrade the NBI power to 6 MW. Two launch options for rf heating

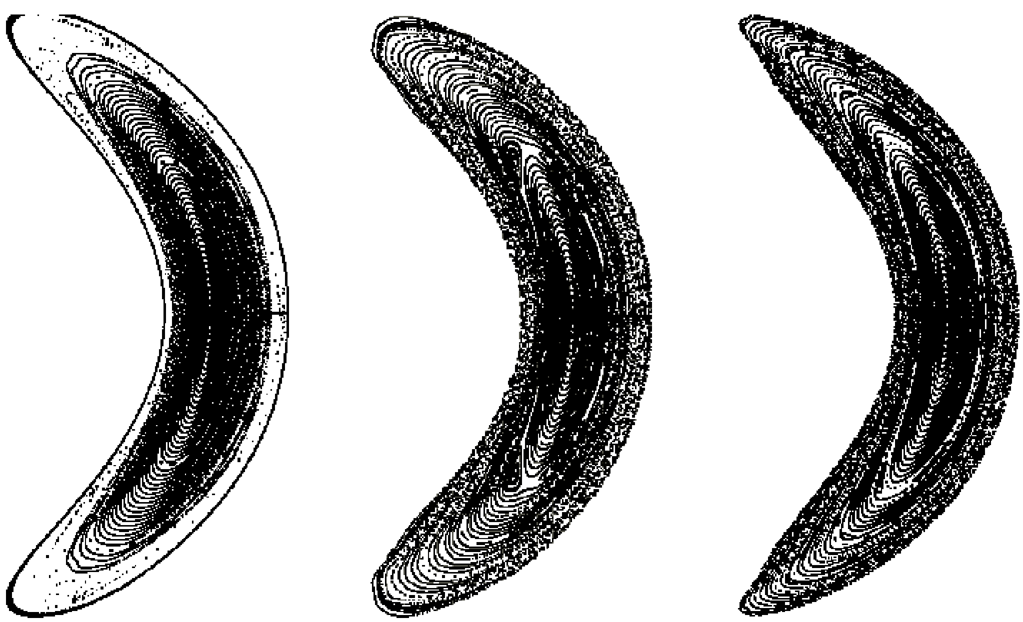

Fig. 5. Poincaré plots of NCSX flux surface cross sections for free-boundary equilibria at vacuum, β = 2%, and β = 4%.

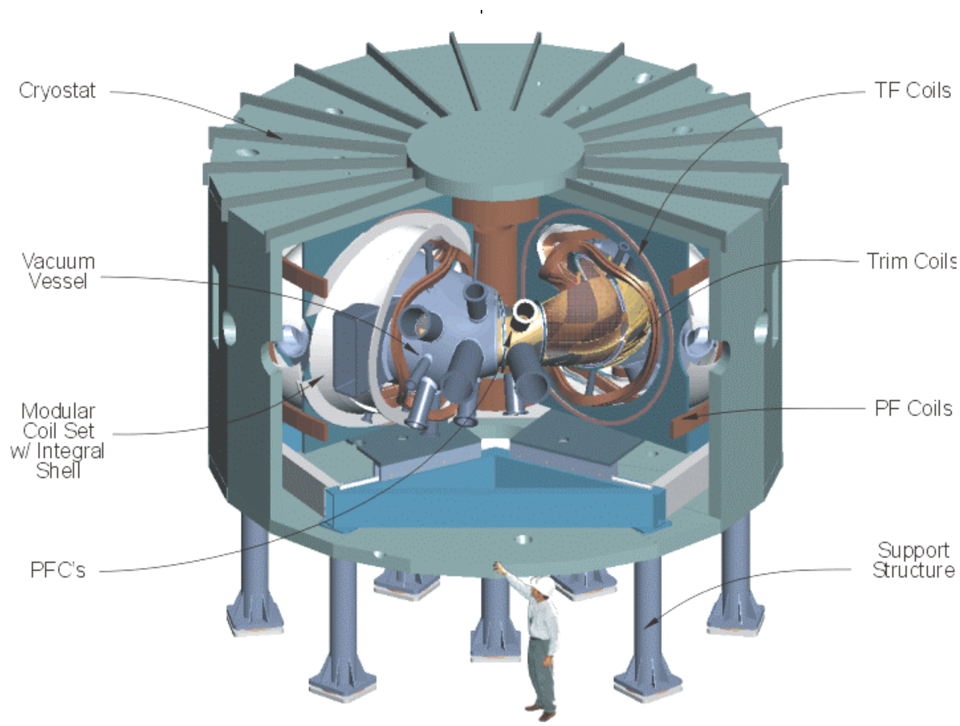

Fig. 6. NCSX stellarator core design.

are available as potential upgrades: mode conversion and high-frequency fast wave. Plasma-facing components will be made of carbon, bakeable in situ to 350° C. A range of internal structures, including neutral beam shinethrough armor, limiters, baffles, divertor, and pumps, are expected to be implemented over the life of the experiment. Fueling will be provided at first by a gas injection system which can provide feedback control on the density; pellet injection will be added later. High vacuum will be provided by an existing turbomolecular pumping system. The facility will be equipped at first with diagnostics needed for shakedown of major machine systems and the first few phases of physics operation, including first-plasma: electron-beam mapping of flux surfaces, Ohmic plasma experiments, and initial heating experiments. More diagnostics will be added during the operating life of the facility. Experimental results from the initial operating phases will help to optimize the selection of new diagnostic systems and their design characteristics.

Engineering Design

The preconceptual engineering design that has been developed for NCSX is built around the 3-period reference plasma configuration, with a major radius of 1.4 m. The plasma is surrounded by a vacuum vessel with an internal structure that can support molded carbon fiber composite (CFC) panels that are bakeable to 350ºC. The design features 21 modular coils, 21 toroidal field coils, and at least 4 pairs of poloidal coils located symmetrically about the horizontal midplane. The coils are pre-cooled to 80 K. A cryostat encloses all of these coils. The modular coils, TF coils, and vacuum vessel are assembled in 120° segments. Each segment features ports for heating, pumping, diagnostics, and maintenance access. A cutaway view of the stellarator core assembly is shown in Fig. 6.

The NCSX will be assembled in the combined PBX/PLT test cell at the Princeton Plasma Physics Laboratory. Many systems formerly used on the PBX, including the neutral beam, vacuum pumping, power supplies, and water systems will be reused. Power supplies formerly used on the Tokamak Fusion Test Reactor (TFTR) will also be used. The cost is expected to be about $65 million. The NCSX project is now in conceptual design. Detailed engineering design is planned to begin in 2002 and construction is to be completed in September 2006.

Conclusions

Compact stellarators provide an important opportunity for the fusion program, offering unique capabilities to advance fusion science and innovative solutions to making magnetic fusion energy more attractive. The QAS builds on the advances in both tokamaks and stellarators and combines the best features of both. A sound physics basis has been established for a proof-of-principle experiment, NCSX, to further develop the physics. The machine concept that has been developed shows that the NCSX scientific mission can be carried out in a practical and affordable facility.

G. H. Neilson
Princeton Plasma Physics Laboratory
Princeton, NJ 08544
E-mail: hneilson@pppl.gov

References

[1] Stellarator Proof of Principle Program, May 11998. http://www.ornl.gov/fed/stelnews/PoP_proposal.pdf

[2] A. H. Boozer, Phys. Fluids **23** (1980) 904.

[3] J. Nührenberg and R. Zille, Phys. Lett. A **129** (1988) 113.

[4] P. Garabedian, Phys. Plasmas **3** (1996) 2483.

[5] V. V. Nemov et al., Phys. Plasmas **6** (1999) 4622.

NCSX Passes Key Reviews

U.S. stellarator researchers' plans to construct the National Compact Stellarator Experiment (NCSX) received a significant boost this Spring with the successful completion of two critical physics reviews. A Department of Energy (DOE) Physics Validation Review (PVR) was conducted 26–28 March 2001, at the Princeton Plasma Physics Laboratory. The fourteen-member peer review committee, chaired by Prof. Gerald Navratil of Columbia University, reviewed the soundness of the NCSX physics basis and physics design approach, using documents and briefings presented by the NCSX design team. In its report, the Navratil committee concluded, “The consensus of the Panel is that the physics requirements and capabilities of the pre-conceptual design of the NCSX experiment represent an appropriate approach to developing the design of a Proof of Principle scale experiment that is the central element in a program to establish the attractiveness of the Compact Stellarator (CS) concept.” The panel found, moreover, that “the choice of the Quasi-Axisymmetric (QAS) approach for a PoP class low aspect ratio, high beta stellarator experiment is appropriate because of its promise of improved confinement and its commonality with the well developed scientific understanding of axisymmetric toroidal plasmas.” The report also made a number of recommendations on design requirements, physics analysis, and management. Following this favorable review, the NCSX project was authorized to proceed with conceptual design, incorporating the review recommendations into its plans. A conceptual design review is planned for the Spring of 2002.

As part of the PVR, a sub-panel of the Fusion Energy Sciences Advisory Committee (FESAC) convened to consider the readiness of the compact stellarator for proof-of-principle (PoP) designation. As a PoP experiment, the NCSX will examine a range of physics issues and provide a physics basis for assessing the attractiveness of the concept. The subpanel, chaired by Prof. Jeffrey Freidberg of the Massachusetts Institute of Technology, found that substantial progress was made in validating the robustness of QAS equilibria over a broad range of profiles, beta values, and start-up scenarios. They found that technical issues identified in an earlier version of the design were resolved in the current NCSX design and as a result they recommended that the compact stellarator be designated a PoP experiment. The full FESAC endorsed this recommendation at its May meeting, citing the compact stellarator's potential to resolve significant issues for fusion energy, to complement existing tokamak and stellarator research, and to advance the science of three-dimensional magnetized plasmas. The FESAC said that the potential fusion gains “earn for the compact stellarator an important place in the portfolio of confinement concepts being pursued by the U.S. Fusion Energy Sciences program.”

The NCSX is jointly proposed by the Princeton Plasma Physics Laboratory and the Oak Ridge National Laboratory in partnership, with other institutions collaborating. To date Auburn University, Columbia University, Lawrence Livermore National Laboratory, New York University, Sandia National Laboratories at Albuquerque, the University of California at San Diego, the University of Texas at Austin, and the University of Wisconsin have collaborated in the physics design. Physicists in Australia, Austria, Germany, Japan, Russia, Spain, Switzerland, and Ukraine have also made vital contributions to the project through international collaboration.

G. H. Neilson
Princeton Plasma Physics Laboratory
Princeton, NJ 08544
E-mail: hneilson@pppl.gov

Status of the QPS Project

The Oak Ridge National Laboratory has developed a proposal for a Quasi-Poloidal Stellarator (QPS). The QPS approach to improving neoclassical transport in stellarators relies on quasi-poloidal symmetry in which there is only a small $\boldsymbol{B} \times \nabla B$ radial drift out of a flux surface. Such configurations can have good neoclassical confinement, high ballooning and kink stability beta limits, and good energetic orbit confinement at the low aspect ratio appropriate for compact stellarator reactors. The device parameters for the proposed QPS experiment are R = 0.9 m, $\langle a \rangle$ = 0.35 m, P(ECRH) = 1 MW, P(ICRF) = 2 MW, and a pulse length of 0.5 s at B = 1 T.

The aims of the QPS experiment are to broaden the understanding of toroidal magnetic configurations through the following tasks:

- study quasi-poloidal symmetry,
- explore very low aspect ratio (~2.6) stellarator configurations,
- contribute to the understanding of physics issues pertinent to a low-*R*/*a*, quasi-poloidal, high-beta compact stellarator concept, and
- complement NCSX in completing the knowledge base needed for advancing the development of the compact stellarator concept to the next stage.

The QPS proposal can be found on the web at
http://qps.fed.ornl.gov/pvr/docment.htm

A Department of Energy (DoE) Physics Validation Review (PVR) of the QPS proposal was conducted 24–25 April 2001 at ORNL. The viewgraphs presented at the review can be found at
http://qps.fed.ornl.gov/pvr/QPSPVRAGN.html.

The PVR committee found that the combination of low aspect ratio and quasipoloidal symmetry is an attractive stellarator option and that the scientific issues of equilibrium, ballooning stability, and transport should be able to be addressed by the proposed experiment. A clear majority of the committee found that these properties fully justify proceeding with the QPS project. A minority felt that the facility should be capable of addressing the question of accessibility of a high-beta regime and, if the confinement and low-beta studies confirm theoretical predictions, the QPS plasma configuration should allow such studies with possible power upgrades. Although a minority of the committee felt that incorporation of a capability to study high-beta access is essential for the QPS project, the majority did not accept this point of view, either finding high beta not critical to QPS or stating that the combination of experimental stability studies at low beta and theoretical analysis will be adequate.

The DOE PVR was successfully passed on May 7, and the QPS project is now in the conceptual design phase. The final plasma and coil configuration will be selected in September and a DOE Conceptual Design, Cost, and Schedule Review is planned for April 2002. As with NCSX, the committee recommended that the decision on whether to proceed with the project should be made within the context of the priority recommendations on a stellarator program to be made by DOE's Fusion Energy Sciences Advisory Committee.

James F. Lyon
Fusion Energy Division, Oak Ridge National Laboratory
P.O. Box 2009
Oak Ridge, TN 37831-8072
E-mail: lyonjf@ornl.gov

MHD activity in high-beta LHD plasmas

In helical plasmas with no net currents, understanding of pressure-driven modes such as resistive/ideal interchange modes and ballooning modes has been a major key issue for realization of high--beta plasmas. In a heliotron configuration, resistive/ideal interchange modes are expected to be unstable because there is a magnetic hill even in high-beta plasmas, even though a magnetic well is formed in the central region by the Shafranov shift. The characteristics of excited instabilities and critical beta value strongly depend on the features of the magnetic configuration. Heliotron-E has strong magnetic shear for stabilization of ideal interchange modes, but there is a strong magnetic hill in the peripheral region. Internal disruptions with particle and energy losses have been triggered by an $m/n = 1/1$ mode in high-beta plasmas with a large pressure gradient [1]. Control of the pressure profile with a strong gas puff flattened the pressure gradient around the $\iota = 1$ surface, and a volume-averaged beta $\langle\beta\rangle$ of 2% was realized by suppression of internal disruptions [2]. In the Compact Helical System (CHS) with large finite-beta effects related to low aspect ratio [3], a volume-averaged equilibrium beta value of 2.1% was achieved when confinement was improved by means of turning off a gas puff [4]. Under these conditions, no strong global instability was observed [5].

Since Large Helical Device (LHD) experiments were started in 1998, plasma parameters have been improved during every experimental campaign by increases in heating power [6]. Recent experiments with high-power neutral beam heating enabled us to obtain $\langle\beta_{dia}\rangle = 3.0\%$ [7], where $\langle\beta_{dia}\rangle$ is estimated by diamagnetic flux measurement and defined as $2\mu_0 \langle p\rangle/B_{av0}^2$, with B_{av0} is the toroidal magnetic field averaged in the outermost flux surface in the vacuum configuration. For realization of high-beta plasmas, a magnetic configuration with inward-shifted magnetic axis R_{ax} has been selected because the neoclassical transport and particle confinement due to high-energy ions are superior to those for the outward-shifted case. However, this configuration produces worse linear MHD stability. The stability beta limits estimated using low-*n* ideal mode analysis and the Mercier criterion are higher for the outward shifted R_{ax} rather than the inward shifted case because of magnetic well formation. Here, observations of MHD activity in high-beta plasmas are reported.

Figure 1 shows the time behavior of a high-beta discharge in a configuration with $R_{ax} = 3.6$ m and a low magnetic field of 0.5 T. Hydrogen gas was supplied by a gas puff and additional fueling is comes from pellet injection at $t = 1.6$ s. The value of $\langle\beta_{dia}\rangle$ increases to 2.6% with gas puff

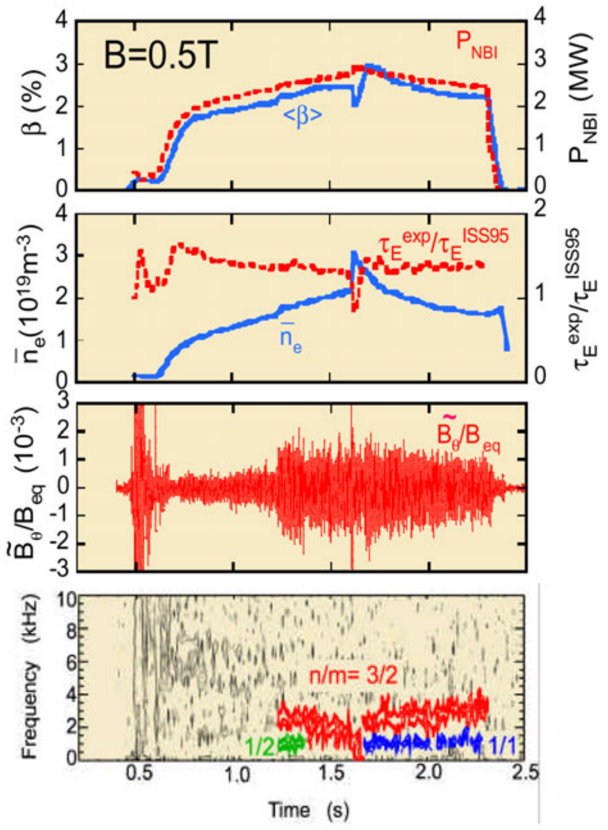

Fig. 1. Time behavior of LHD high-beta discharge in a configuration with R_{ax} = 3.6 m and B_t = 0.5 T.

fueling and reaches 3.0% with pellet injection. The energy confinement time normalized by the ISS95 scaling is maintained around 1.4 throughout the discharge. In the magnetic fluctuation measurements, coherent modes with m/n = 2/1, 1/1, and 2/3 were observed. The m/n = 2/3 and 1/1 modes excited near the outermost surface are predominant when $\langle\beta_{dia}\rangle > 2.2\%$. In contrast, the m/n = 2/1 mode in the core region disappears when $\langle\beta_{dia}\rangle > 2.2\%$. Although the $\langle\beta_{dia}\rangle$ signal has a synchronized fluctuation with m/n = 2/3 mode, the effect on global energy confinement $\Delta\beta/\beta$ is less than 5%. Violent MHD activity that terminates the plasma has not been observed so far.

In previous experiments, a pedestal structure has been observed. Its presence has made a great contribution to global plasma confinement [8,9], and the structure has formed a large pressure gradient in the peripheral region with a magnetic hill. Stability against ideal interchange modes is guaranteed by a strong magnetic shear. On the other hand, the core region can be unstable because of weak magnetic shear although the pressure gradient is qualitatively low. Figure 2 shows the changes of the pressure gradient at ρ = 0.5, which roughly corresponds to the location of the ι = 1/2 rational surface, as a function of $\langle\beta_{dia}\rangle$. The regimes of Mercier instability and low-n mode

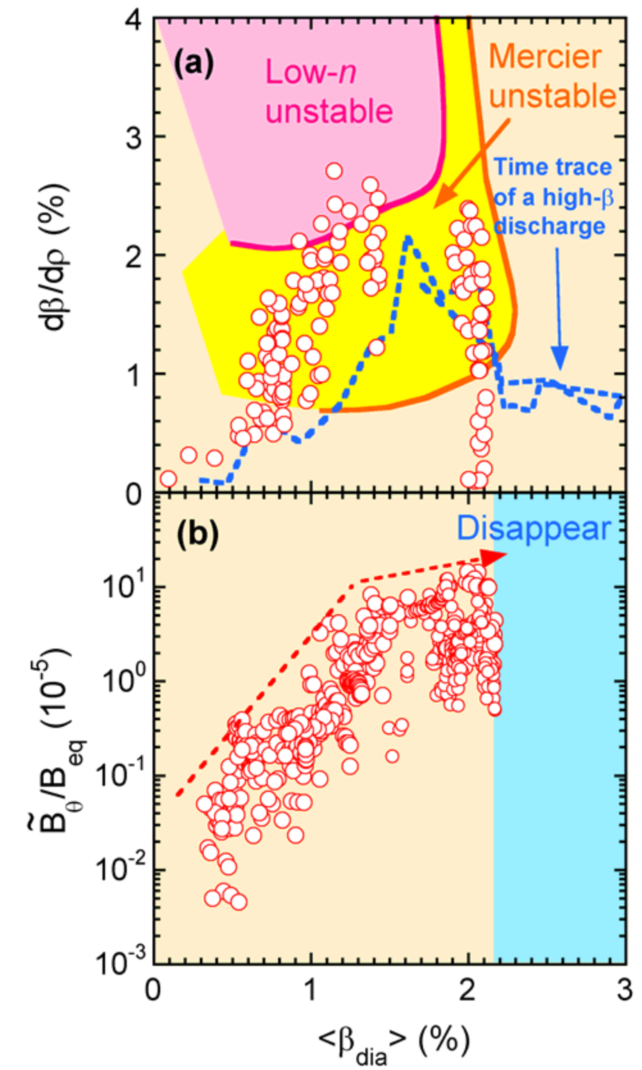

Fig. 2. Changes in (a) pressure gradient at ρ = 0.5 and (b) fluctuation amplitude of m/n = 2/1 mode as a function of $\langle\beta_{dia}\rangle$.

instabilities are also illustrated. The stability of low-n modes is calculated using the three-dimensional MHD stability analysis code TERPSICHORE [10]. In this case, the pressure gradient already exceeds the Mercier criterion and is deep into the low-n mode unstable region.

When a large pressure gradient, deep in the low-n mode unstable region, is formed temporarily by pellet injection, minor relaxation phenomena have sometimes been observed [11] at a major rational surface in the core region. Many experimental points with quite a low-pressure gradient are seen around $\langle\beta_{dia}\rangle$ of 2% in Fig. 2(a). These points correspond to occasional local flattening, which suggests formation of an m/n = 2/1 island [12]. The change in fluctuation amplitude of the m/n = 2/1 mode is shown in Fig. 2(b). The m/n = 2/1 mode located in the core region also appears with a threshold $\langle\beta_{dia}\rangle$ of about 0.3%.

Although the amplitude increases with the pressure gradient, it saturates with when $\langle\beta_{dia}\rangle$ exceeds about 1.3%. The $m/n = 2/1$ mode has not been observed when $\langle\beta_{dia}\rangle > 2.2\%$. A time trace of the same high-beta discharge of Fig.1 indicates that the pressure gradient evolves roughly along with the envelope of a set of data up to $\langle\beta_{dia}\rangle$ of 2%. That is, the time trace of an individual shot roughly follows the collection of data from many shots that is shown by the circles in Fig. 2. However, the pressure gradient decreases with $\langle\beta_{dia}\rangle$ above that. If the pressure gradient is suppressed by the interchange mode, it should recover and grow further in the second stability regime. However, experimental observation shows that the pressure gradient does not develop further. In addition to a detailed investigation of stability, the transport and power deposition in this particular low magnetic field operation should be considered.

At the edge point of $\rho = 0.9$, which roughly corresponds to the $\iota = 1$ surface, both the local pressure gradient and the amplitudes of coherent resonant modes evolve monotonically with $\langle\beta_{dia}\rangle$, as shown in Fig. 3. Although this radius has often been discussed in relation to the generation of a magnetic island [13], flattening due to the island has not been observed at low magnetic field operation within the spatial resolution of the Thomson scattering diagnostic (~2.5 cm). A pressure gradient greater than the Mercier criterion has been obtained here as well as in the case of $\rho = 0.5$.

S. Sakakibara for LHD Experimental Group
National Institute for Fusion Science
Oroshi-cho 322-6, Toki 509-5292, Japan
E-mail: sakakis@LHD.nifs.ac.jp

References

[1] J. H. Harris et al., Phys. Rev. Lett. **53** (1984) 2242.

[2] O. Motojima et al., Nucl. Fusion **25** (1985) 1783.

[3] H. Yamada et al., in Proc. 14th Int. Conf. on Plasma Physics and Controlled Nuclear Fusion Research 1992, Vol. 2, IAEA, Vienna (1993) 493.

[4] S. Okamura et al., Nucl. Fusion **35** (1995) 283.

[5] S. Sakakibara et al., J. Phys. Soc. Jpn. **63** (1994) 4406.

[6] O. Motojima et al. Phys. Plasmas **6** (1999) 1843.

[7] H. Yamada et al., submitted to Plasma Phys. Controlled. Fusion.

[8] H. Yamada et al., Phys. Rev. Lett. **84** (2000) 1216.

[9] N. Ohyabu et al., Phys. Rev. Lett. **84** (2000) 103.

[10] W. A. Cooper et al., Plasma Phys. Controlled Fusion **34** (1992) 1011.

[11] K. Toi et al., in the Proc. 27th EPS Conf. on Controlled Fusion and Plasma Physics, Budapest, 2000.

[12] S. Sakakibara et al., Nucl. Fusion (in press).

[13] N. Ohyabu et al., Phys. Plasmas **7** (2000) 1802.

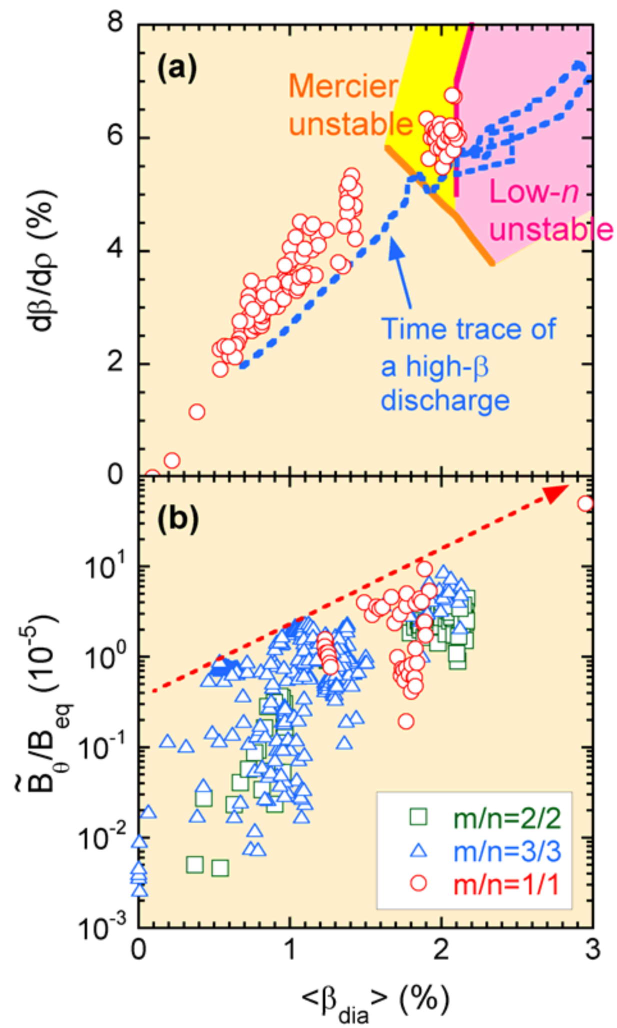

Fig. 3. Changes in (a) pressure gradient at $\rho = 0.9$ and (b) fluctuation amplitudes of $\iota = 1$ resonant modes as a function of $\langle\beta_{dia}\rangle$.